Supplement of Earth Syst. Sci. Data, 16, 5207–5226, 2024
https://doi.org/10.5194/essd-16-5207-2024-supplement

Open Access Earth System Science Data

Supplement of

CIrrMap250: annual maps of China's irrigated cropland from 2000 to 2020 developed through multisource data integration

Ling Zhang et al.

Correspondence to: Ling Zhang (zhanglingky@lzb.ac.cn)

1 Supplementary Figures

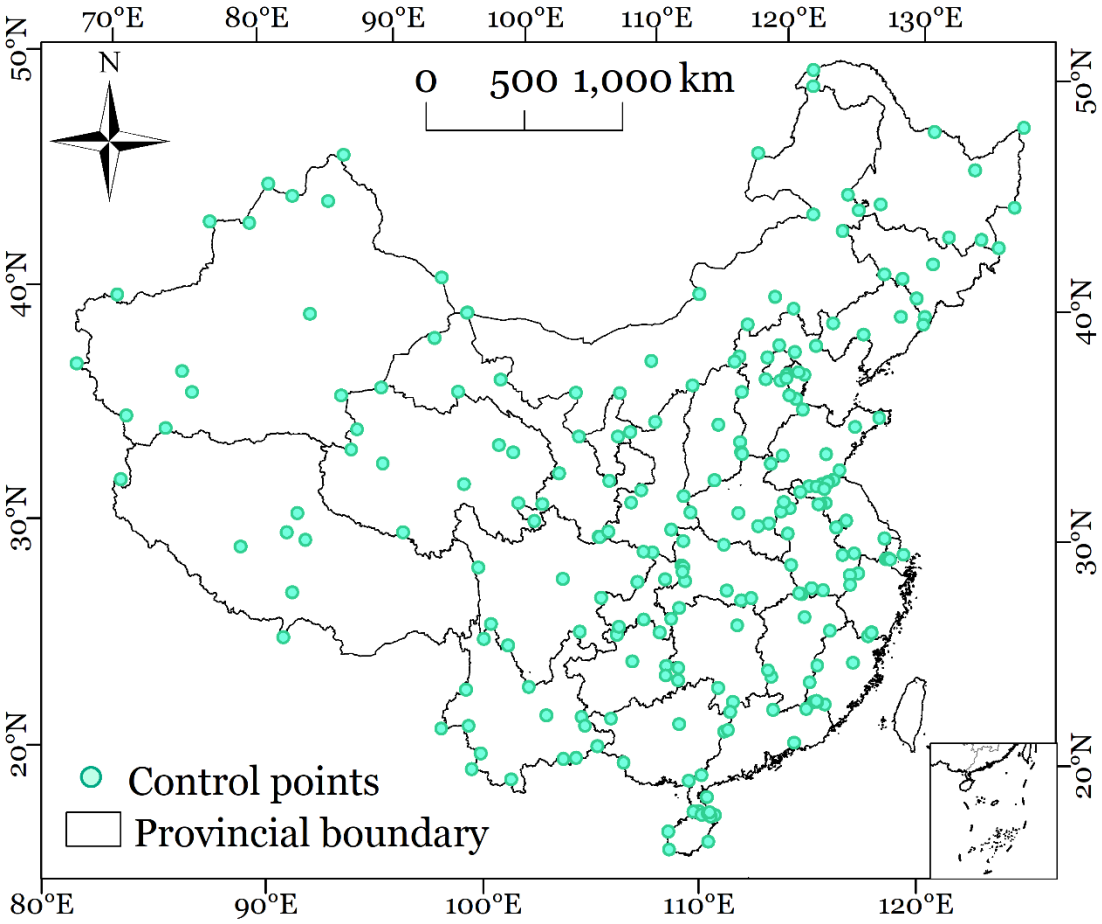

Figure S1. Spatial distribution of the identified reference points used for georeferencing the land-use maps of China's second National Land Survey

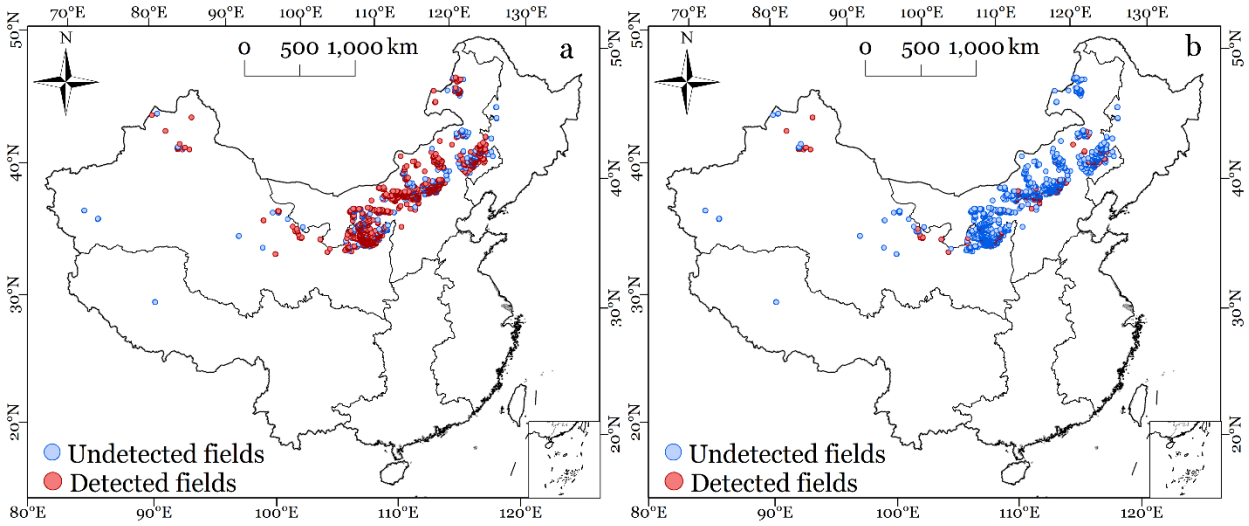

Figure S2. Spatial distribution of the detected and undetected fields with center pivot irrigation systems for the year 2020. Panels a and b show the results of CIrrMap250 and IrriMap_CN, respectively.

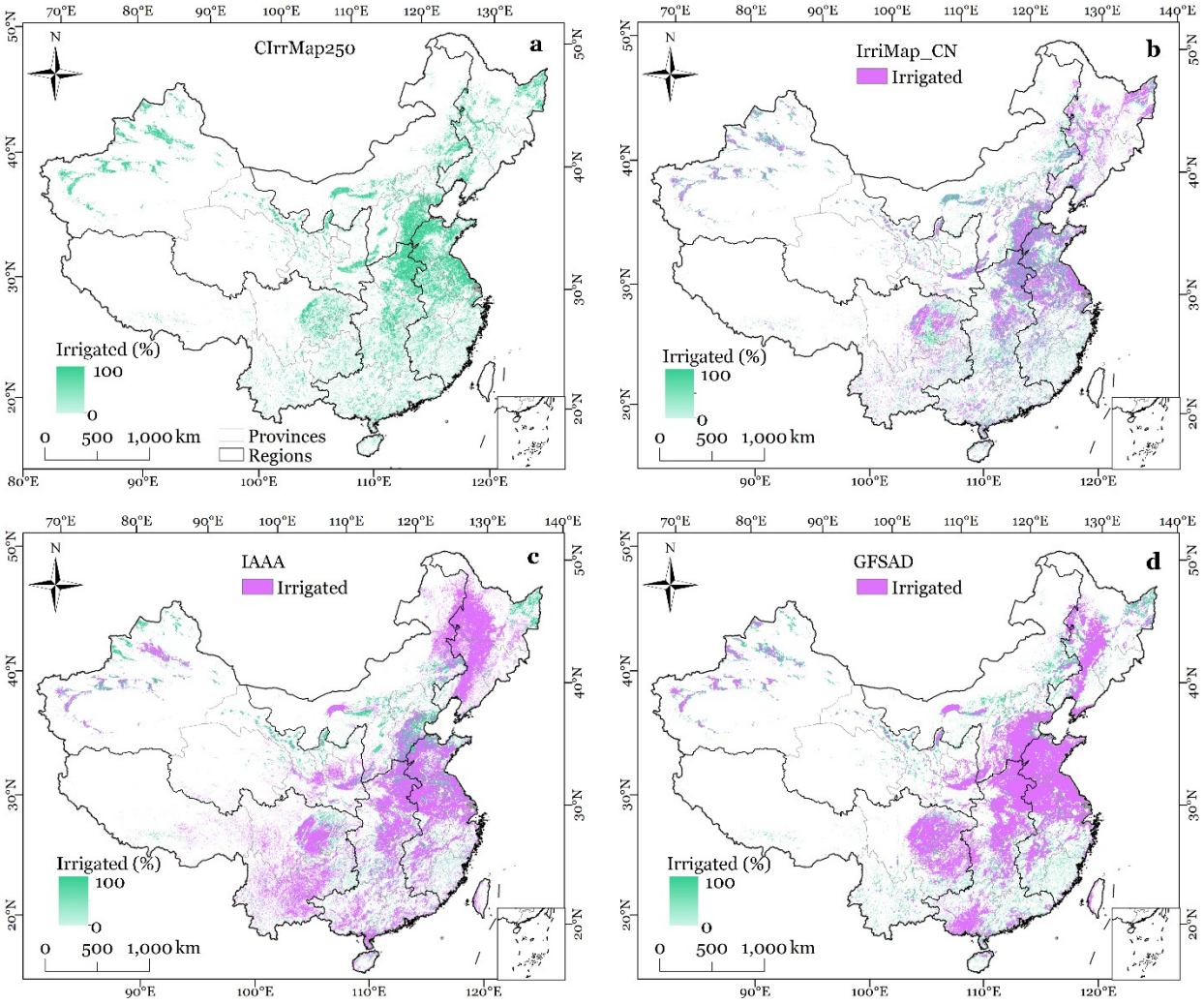

Figure S3. Comparison of irrigated cropland distribution from CIrrMap250 with existing products (IrriMap_CN, IAAA, GFSAD) for the year 2010. Panel a shows the spatial distribution of irrigated cropland from CIrrMap250, while panels b, c, and d overlay the existing binary maps IrriMap_CN, IAAA, and GFSAD on CIrrMap250, respectively.

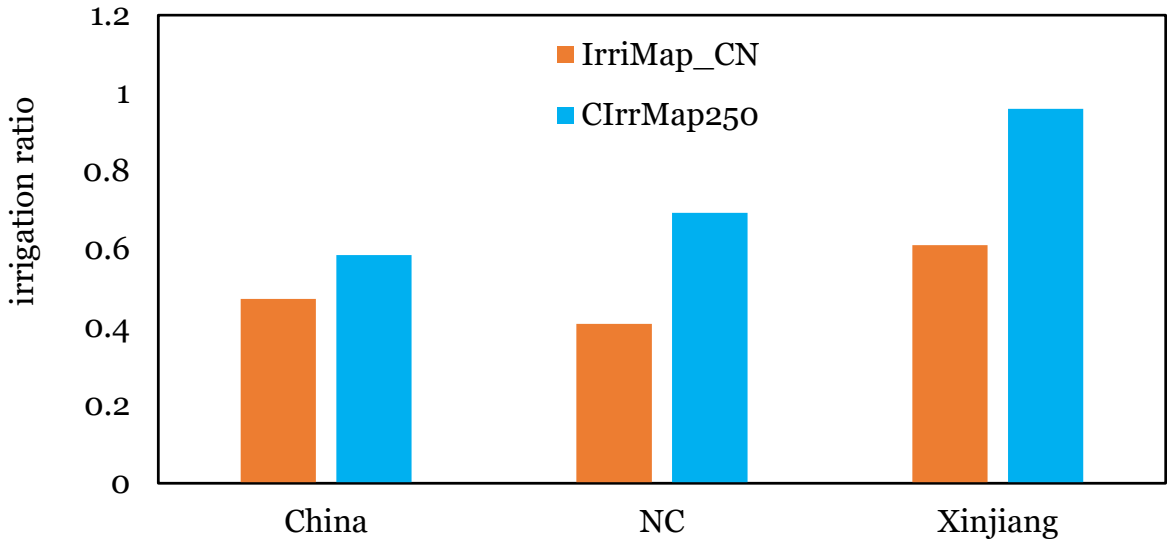

Figure S4. Comparison of irrigated ratio estimates of CIrrMap250 and IrriMap_CN in China, Northern China, Xinjiang Uygur Autonomous Region

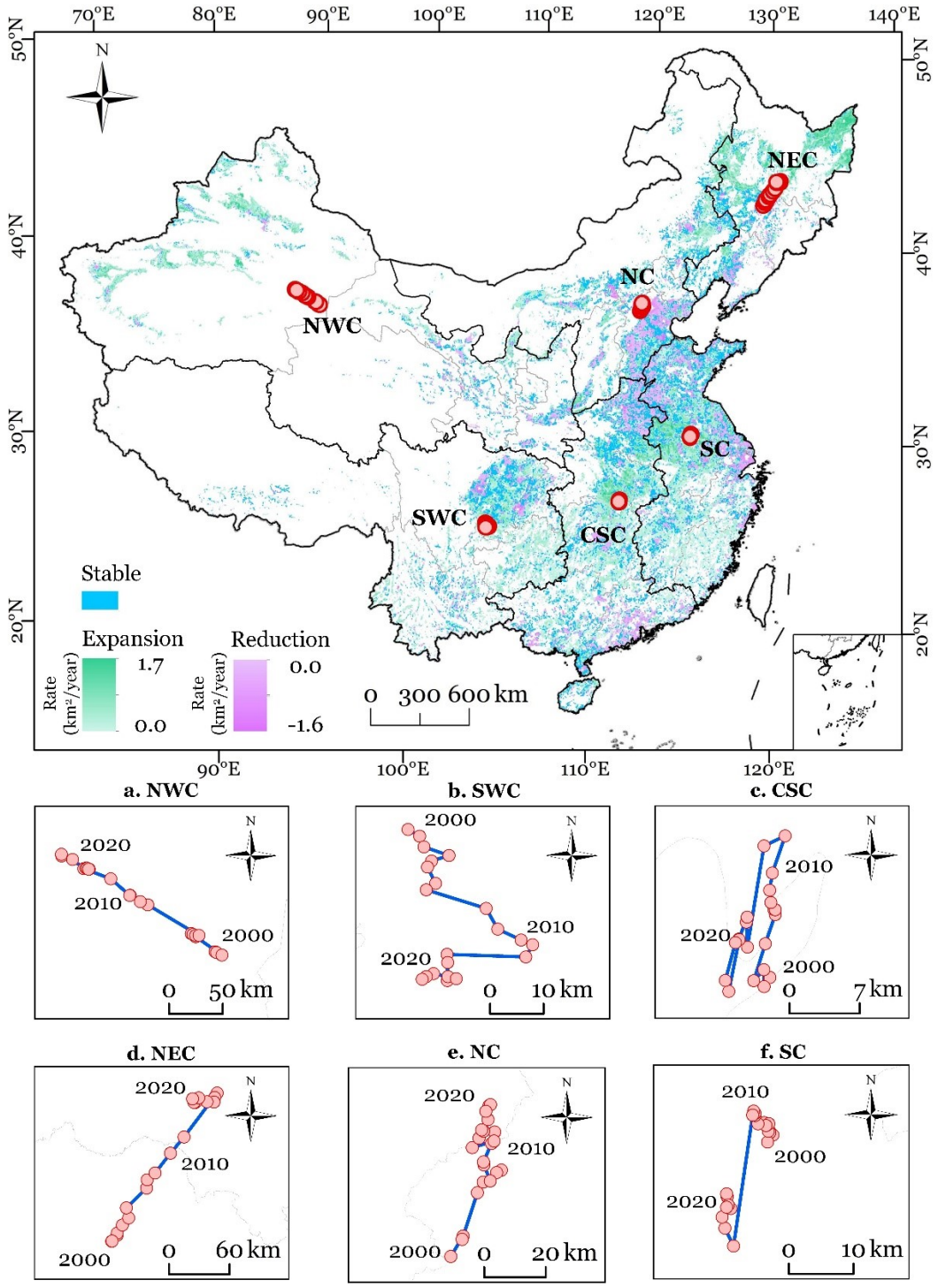

Figure S5. Spatial trends in irrigated areas from 2000 to 2020 in the six subregions of China. The top panel shows the interannual trend in irrigated area at the pixel scale (same as Figure 8 in the main text) and illustrates the locations of the gravity centers of irrigated areas for each subregion. Panels a-d depict the center-of-gravity movement of irrigated areas from 2000 to 2020 in each subregion.

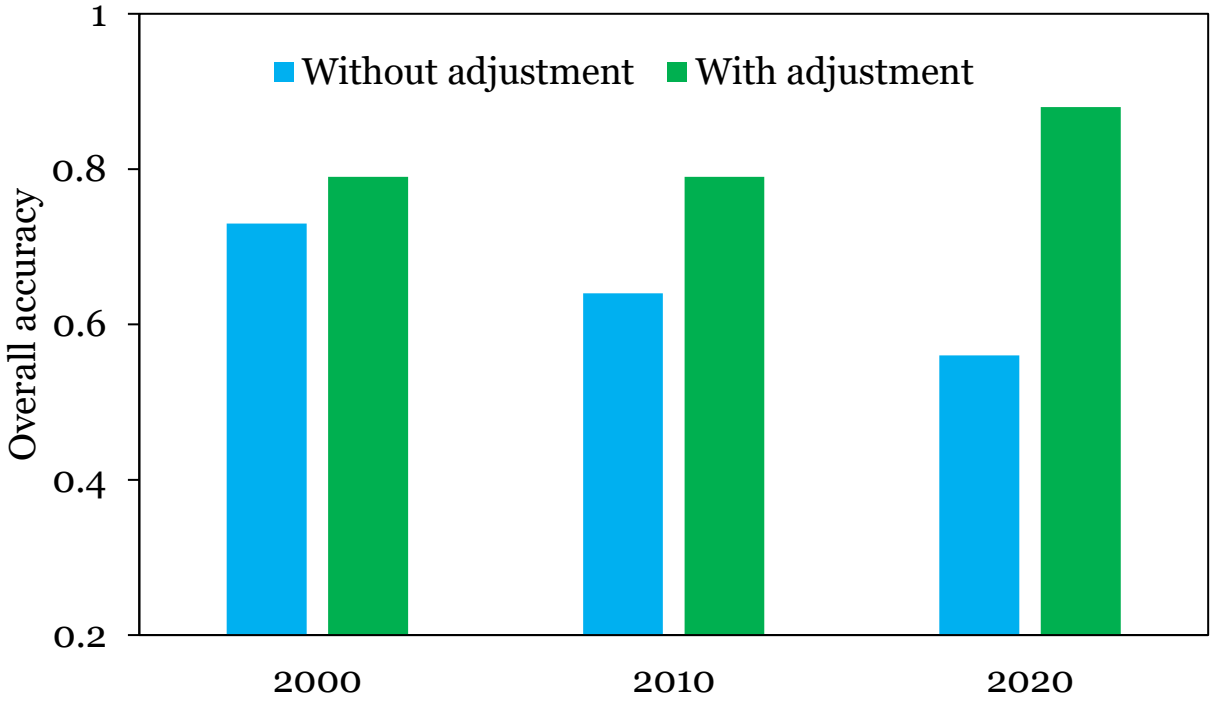

Figure S6. Comparison of the performance of irrigation maps constrained by different irrigated area data. "without adjustment" means the use of the original irrigation statistics, while "with adjustment" indicates the use of the harmonized and reconciled irrigated areas (this study).

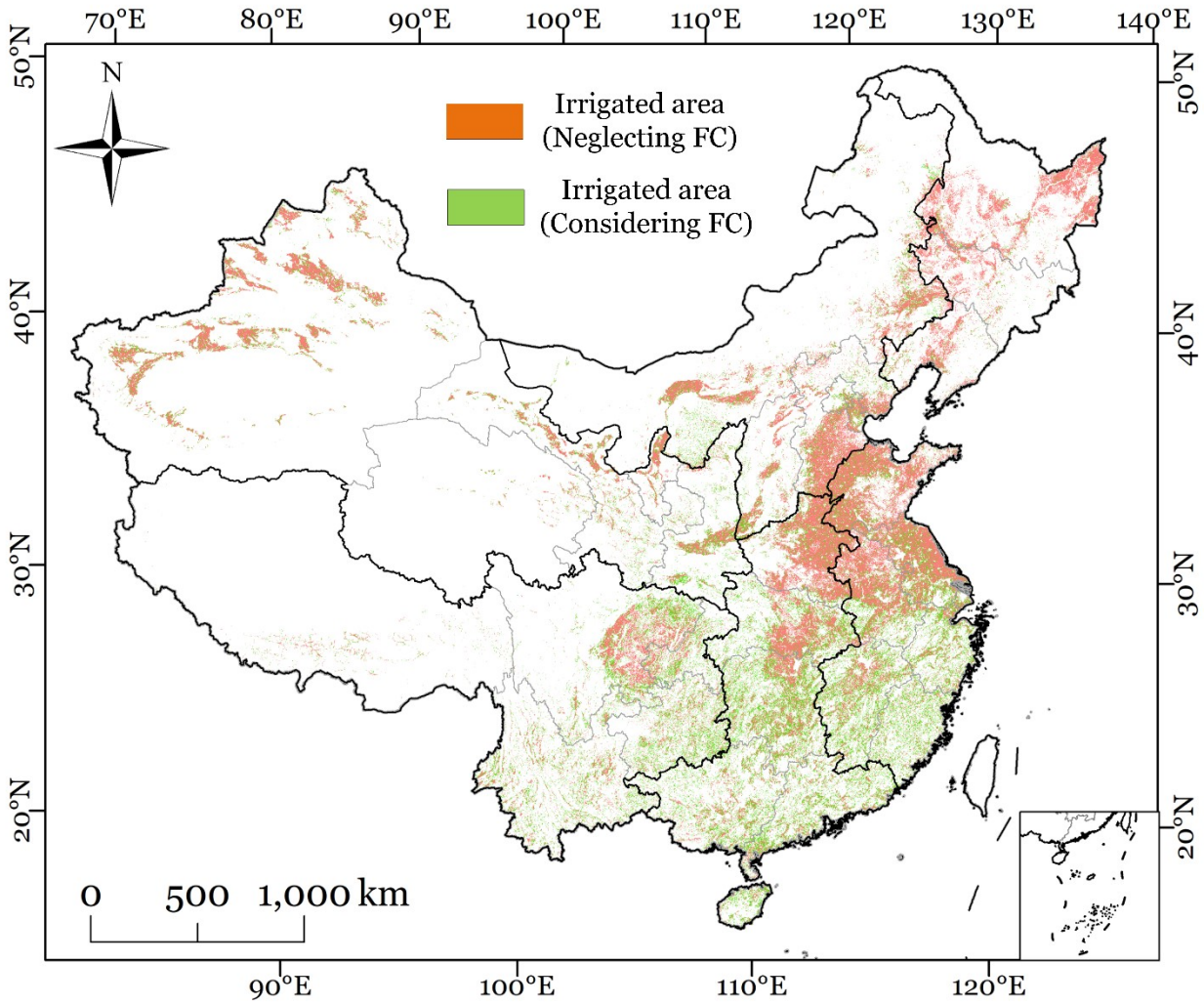

Figure S7. Comparison of irrigated area distribution in the scenarios of considering fractional coverage (FC) of cropland (this study) and neglecting FC of cropland

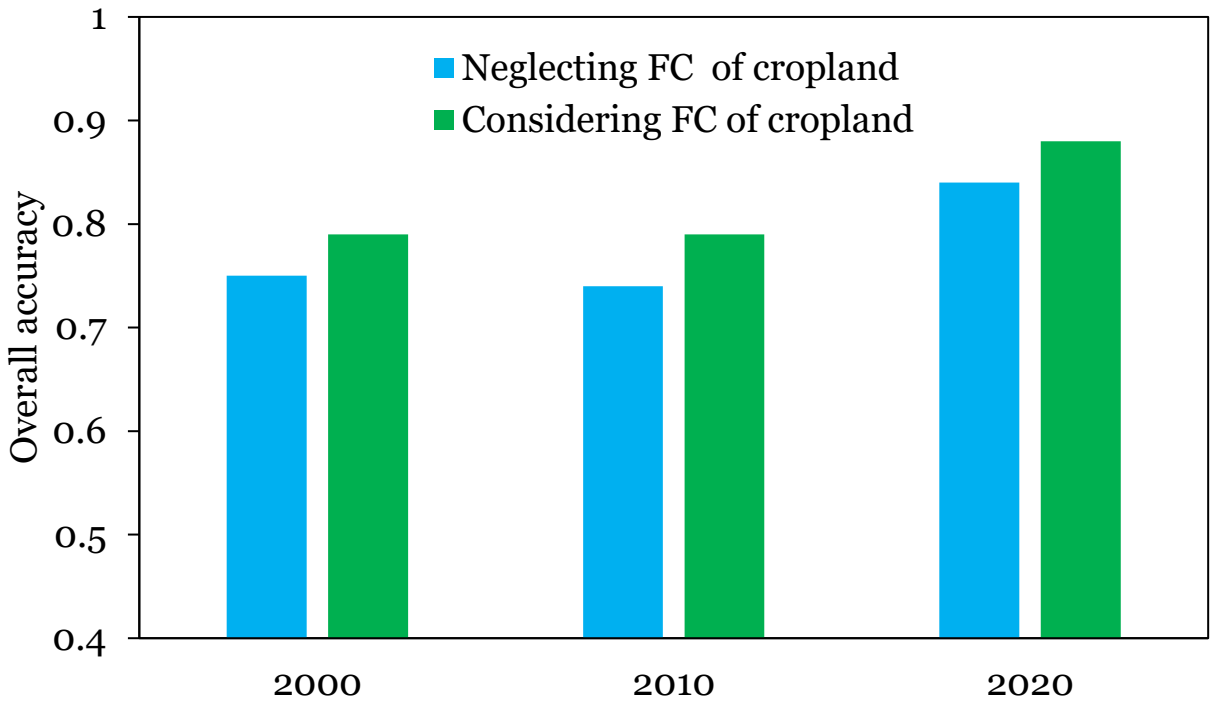

Figure S8. Comparison of performance of irrigation maps in the scenarios of considering fractional coverage (FC) of cropland (this study) and neglecting FC of cropland

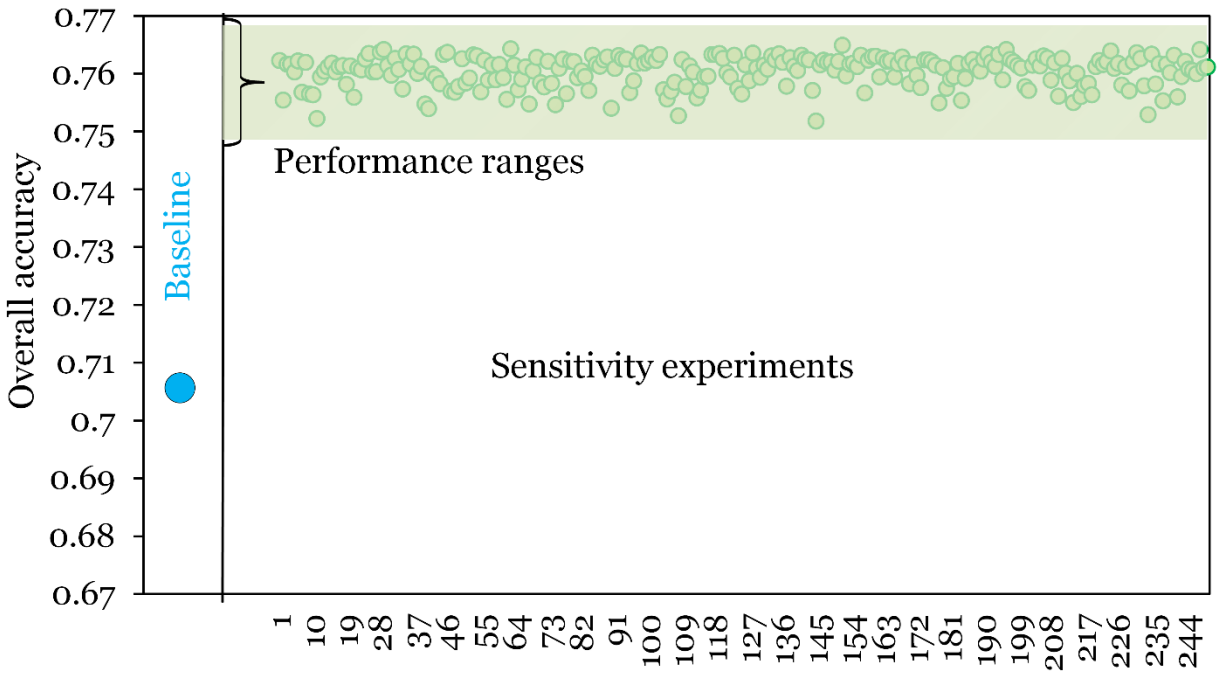

Figure S9. Sensitivity analysis of irrigation map performance to the use of different irrigation suitability maps. The performance of these irrigation maps was compared with the baseline irrigation map, which was created by the method in our study but disregarded irrigation suitability during the mapping process.

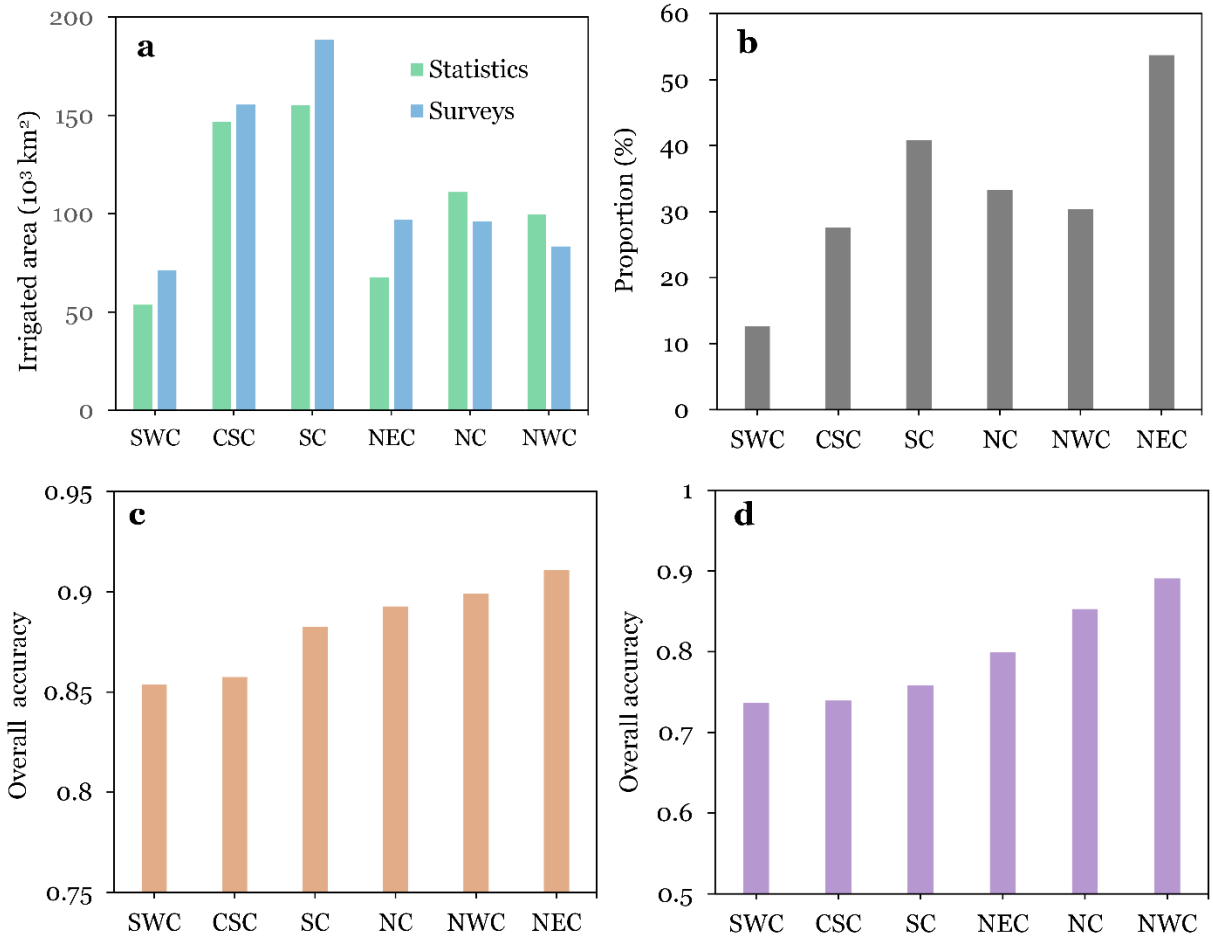

Figure S10. Uncertainty analysis of the CIrrMap250 product. a. Comparison of statistics and surveys of irrigated area across different subregions. **b**. Proportion of croplands consistently identified by five state-of-the-art remote sensing land use/cover products, including GlobeLand30 (Chen et al., 2015), GLAD (Potapov et al., 2021), CLUD (Liu et al., 2014), CLCD (Yang and Huang, 2021), and CACD (Yu et al., 2021). **c**. Comparison of the accuracy of the hybrid cropland product CCropLand30 across different subregions. **d**. Comparison of the accuracy of CIrrMap250 (for the year 2010) across different subregions.

2 Supplementary Tables

Table S1. Summary of MODIS-derived vegetation indices used in this study

Vegetation indices	Formula	MODIS bands	Resolution
NDVI	(NIR - Red) / (NIR + Red)	Band 01 (Red) Band 02 (NIR)	250 m/16 day
EVI	2.5*(NIR-Red) / (NIR+ 6*Red–7.5*Blue+1)	Band 01 (Red) Band 02 (NIR) Band 03 (Blue)	250 m/16 day
GI	NIR/Green	Band 02 (NIR) Band 04 (Green)	250 m/8 day

where NIR is the near-infrared band (841-876 nm); and Red (620-670 nm), Blue (459-479 nm) and Green (545 – 565 nm) are the visible red band, visible blue band, and visible green band, respectively.

Table S2. Summary of the products and variables used in this study

Product /variable	Description	Formula	Source
CCropLand30	Hybrid cropland product for China	—	Zhang et al. (2024)
CLUD	China's Land-use/cover dataset	—	Liu et al. (2014)
NDVI/EVI/GI	Normalized Vegetation Index / Enhanced Vegetation Index / Greenness Index	See Table S1	MODIS[a]
Irrigation suitability	Suitability of cropland for irrigation	Equation 4 in the main text	PWRD[d]
SVI	Irrigation suitability-adjusted peak vegetation index	Equation 5 in the main text	This study[b]
Precipitation	Annual precipitation	$\sum_{i=1}^{Ydays} PCP_i$	NMIC[c]
Temperature	Mean annual temperature	$\frac{1}{Ydays}\sum_{i=1}^{Ydays} TMP_i$	NMIC[c]
PET	Annual evapotranspiration	$\sum_{i=1}^{Ydays} PET_i$	This study[b]
Aridity index	Degree of dryness of the climate	MA_PCP/MA_PET	This study[b]
Irrigation water withdrawal	Total amount of water withdrawals used for crop irrigation	—	This study[b]
WSI	Water scarcity index	TWU/WA	Zhang et al. (2023)
Cropping intensity	Number of crops grown on the same field in a given agricultural year	—	Xu et al. (2017)
Soil type	Genetic soil classification system in China	—	RESDC[e]

Elevation	Mean elevation	—	SRTM[f]
Slope	Mean slope	—	This study[b]
Distances to water bodies	Euclidean distance to rivers, lakes, reservoirs, canals, and ponds	—	This study[b]

Note. [a]indicates variables derived from Moderate Resolution Imaging Spectroradiometer (MODIS) data (https://modis.gsfc.nasa.gov/). [b]indicates variables generated in this study. [c]indicates the National Meteorological Information Center (http://data.cma.cn/). [d]indicates the provincial water resources departments. [e]indicates the Resource and Environment Science and Data Center (https://www.resdc.cn/Default.aspx). [f]indicates the Shuttle Radar Topography Mission (https://www.earthdata.nasa.gov/sensors/srtm). *Ydays* represents the number of days in a given year; PCP_i denotes the amount of precipitation at the i^{th} day; TMP_i indicates mean air temperature at the i^{th} day; PET_i represents evapotranspiration estimated using the Priestley-Taylor method (Priestley and Taylor, 1972); *MA_PCP* and *MA_PET* denote mean annual precipitation and PET, respectively; *TWU* represents total water use, including both groundwater and surface water withdrawals for irrigation, industry, domestic purposes, forestry, livestock, and fishery; *WA* represents water availability and refers to the total surface water and groundwater generated by precipitation.

Table S3. Suitability values for the influencing factors of irrigation suitability

Influencing factors	Reclassification	Suitability value
elevation	S1: < min+100	S1=4
	S2: [min+100, min+300]	S2=3
	S3: [min+300, min+500]	S3=2
	S4: > min+500	S4=1
slope	S1: <2%	S1=4
	S2: [2%, 4%]	S2=3
	S3: [4%, 8%]	S3=2
	S4: > 8%	S4=1
aridity index	S1: <0.1	S1=10
	S2: [0.1, 0.2]	S2=9
	S3: [0.2, 0.3]	S3=8
	S4: [0.3, 0.4]	S4=7
	S5: [0.4, 0.5]	S5=6
	S6: [0.5, 0.6]	S6=5
	S7: [0.6, 0.7]	S7=4
	S8: [0.7, 0.8]	S8=3
	S9: [0.8, 0.9]	S9=2
	S10: >0.9	S10=1

Note: min is minimum elevation of the mapping unit

Table S4. Optimized hyperparameters of the random forest algorithm

Hyperparameters	Descriptions	values
Ntree	Number of trees	200
MinObs	Minimum number of observations per node	10
Nsplit	Number of variables randomly sampled at each decision split	7

Table S5. Definitions of the performance metrics

Metrics	Formula	Variables
Overall accuracy	$\frac{\sum_{i=1}^{n} P_{ii}}{N}$	n is the number of classes; P_{ii} is the number of pixels on row i and column i in the confusion matrix, which represent the total number of pixels correctly classified; N is total number of pixels used for accuracy evaluation; P_{i+} and P_{+i} are the total number of pixels on row i (observations) and column i (predictions), respectively.
F1-score	$2\frac{\frac{P_{ii}}{P_{+i}} \times \frac{P_{ii}}{P_{i+}}}{\frac{P_{ii}}{P_{+i}} + \frac{P_{ii}}{P_{i+}}}$	
Producer's accuracy	$\frac{P_{ii}}{P_{+i}}$	
User's accuracy	$\frac{P_{ii}}{P_{i+}}$	

Table S6. Performance metric values of CIrrMap250 and existing maps (IrriMap_CN, IAAA, GFSAD). OA, PU, UA represent overall accuracy, producer's accuracy, and user's accuracy, respectively.

Year	Products	OA	F1-score	Irr PA	Irr UA	NIrr PA	Nirr UA
2000	CIrrMap250	0.79	0.78	0.80	0.78	0.77	0.79
	IrriMap_CN	0.68	0.73	0.51	0.80	0.87	0.63
	IAAA	0.55	0.50	0.66	0.56	0.45	0.55
2010	CIrrMap250	0.79	0.71	0.83	0.83	0.71	0.71
	IrriMap_CN	0.66	0.62	0.61	0.81	0.75	0.53
	IAAA	0.61	0.50	0.64	0.71	0.54	0.46
	GFSAD	0.59	0.51	0.60	0.71	0.58	0.46
2020	CIrrMap250	0.88	-	0.88	1	-	-
	IrriMap_CN	0.20	-	0.20	1	-	-

Note. CIrrMap250 and IrriMap_CN achieves a perfect user's accuracy for the irrigation class in 2020 because all the reference points are irrigated samples.

Table S7. Confusion matrix for CIrrMap250 and existing maps (IrriMap_CN, IAAA, GFSAD) in 2000, 2010, and 2020, respectively

	Products	Classified	Reference	
			Irrigated	Non-irrigated
2000	CIrrMap250	Irrigated	271	75
		Non-irrigated	66	246
	IrriMap_CN	Irrigated	172	43
		Non-irrigated	165	278
	IAAA	Irrigated	221	177
		Non-irrigated	116	144
	Products	Classified	Reference	
			Irrigated	Non-irrigated
2010	CIrrMap250	Irrigated	6818	1385
		Non-irrigated	1365	3325
	IrriMap_CN	Irrigated	5003	1167
		Non-irrigated	3180	3543
	IAAA	Irrigated	5274	2183
		Non-irrigated	2909	2527
	GFSAD	Irrigated	4939	1995
		Non-irrigated	3244	2715
	Products	Classified	Reference	
			Irrigated	Non-irrigated
2020	CIrrMap250	Irrigated	6340	0
		Non-irrigated	849	0
	IrriMap_CN	Irrigated	1426	0
		Non-irrigated	5763	0

References

Chen, J., Chen, J., Liao, A., Cao, X., Chen, L., Chen, X., He, C., Han, G., Peng, S., Lu, M., Zhang, W., Tong, X., Mills, J., 2015. Global land cover mapping at 30m resolution: A POK-based operational approach. ISPRS Journal of Photogrammetry and Remote Sensing, 103: 7-27. DOI:10.1016/j.isprsjprs.2014.09.002

Liu, J., Kuang, W., Zhang, Z., Xu, X., Qin, Y., Ning, J., Zhou, W., Zhang, S., Li, R., Yan, C., Wu, S., Shi, X., Jiang, N., Yu, D., Pan, X., Chi, W., 2014. Spatiotemporal characteristics, patterns, and causes of land-use changes in China since the late 1980s. Journal of Geographical Sciences, 24(2): 195-210. DOI:10.1007/s11442-014-1082-6

Priestley, C. H. B. and Taylor, R. J.: On the Assessment of Surface Heat Flux and Evaporation Using Large-Scale Parameters, Monthly Weather Review, 100, 81-92, 10.1175/1520-0493(1972)100<0081:OTAOSH>2.3.CO;2, 1972.

Potapov, P., Turubanova, S., Hansen, M.C., Tyukavina, A., Zalles, V., Khan, A., Song, X.-P., Pickens, A., Shen, Q., Cortez, J., 2021. Global maps of cropland extent and change show accelerated cropland expansion in the twenty-first century. Nature Food. DOI:10.1038/s43016-021-00429-z

Xu, X., 2017. Remote sensing-derived crop intensity for China's cropland (in Chinese). http://www.resdc.cn. DOI:10.12078/2017122201

Yang, J., Huang, X., 2021. The 30 m annual land cover dataset and its dynamics in China from 1990 to 2019. Earth System Science Data, 13(8): 3907-3925. DOI:10.5194/essd-13-3907-2021

Yu, Z., Jin, X., Miao, L., Yang, X., 2021. A historical reconstruction of cropland in China from 1900 to 2016. Earth System Science Data, 13(7): 3203-3218. DOI:10.5194/essd-13-3203-2021

Zhang, L., Ma, Q., Zhao, Y., Chen, H., Hu, Y., and Ma, H.2023. China's strictest water policy: Reversing water use trends and alleviating water stress, Journal of Environmental Management, 345, 118867, 10.1016/j.jenvman.2023.118867

Zhang, L., Wang, W., Ma, Q., Hu, Y., and Zhao, Y. 2024. CCropLand30: High-resolution hybrid cropland maps of China created through the synergy of state-of-the-art remote sensing products and the latest national land survey, Computers and Electronics in Agriculture, 218, 108672, 10.1016/j.compag.2024.108672